Temperature scales of magnetization oscillations in an asymmetric quantum dot

E. N. Bogachek, A. G. Scherbakov, and Uzi Landman

School of Physics, Georgia Institute of Technology, Atlanta, Georgia 30032-0430
(Received 22 September 2000; published 2 March 2001)

The temperature scales of different types of magnetization oscillations in a quantum dot, formed in a two-dimensional electron gas by circularly symmetric or asymmetric confining potentials, are studied. Aharonov-Bohm (AB) oscillations, with a superimposed fine structure caused by magnetic-field-induced shifts of the electronic energy levels, develop at low magnetic fields $\omega_c \ll \omega_{x,y}$ (where ω_c is the cyclotron frequency and $\omega_{x,y}$ are the harmonic confining frequencies that determine the shape and effective size of the dot). The characteristic scale of the fine-structure fluctuations is $\phi_0/(\varepsilon_F/\hbar\omega_0)$ (where ϕ_0 is the flux quantum, ε_F is the Fermi energy, and $\omega_0 = \sqrt{\omega_x \omega_y}$) and they are smeared at temperatures $T > (\hbar\omega_0)^2/\varepsilon_F$, with restoration of the pure AB picture for $T \lesssim \hbar\omega_0$. At high magnetic fields, $\omega_c \gg \omega_{x,y}$, de Haas–van Alphen oscillations develop (for $T \lesssim \hbar\omega_c$), with a superimposed AB oscillatory structure which undergoes temperature smearing for $T \gtrsim \hbar\omega_0(\omega_0/\omega_c)$. Effects of the asymmetry of the confining potential on the magnetization oscillations are discussed. The magnetic moment of the dot as a function of the chemical potential exhibits a series of paramagnetic peaks superimposed on a diamagnetic background, and the influence of the magnetic-field strength and asymmetry of the dot on these features is discussed.

I. INTRODUCTION

The behavior of metallic and semiconducting systems under the influence of magnetic fields may exhibit new features in the submicron range when the system's size becomes comparable to the typical length of the electronic trajectory in it. In sufficiently small systems coherent motion of the electrons may be achieved, and this leads to the appearance of new quantum phenomena. One of the most interesting effects occurring in such systems under appropriate conditions is the Aharonov-Bohm (AB) effect. Predicted first for electron beams in vacuum,[1] the AB effect may be realized, as found theoretically[2] and subsequently demonstrated in experiments on bismuth wiskers,[3] in simply connected solids. In such systems the character of the motion of the electrons near the boundaries changes significantly, resulting in the formation of a new type of electronic states localized near the surface. Such surface states form whispering gallery states in the case of weak magnetic fields,[2] i.e., when $r_c \gg a$ (where r_c is the cyclotron radius corresponding to the cyclotron frequency ω_c, and a is the size of the system), or edge states in the opposite case of a strong magnetic field (see, e.g., Ref. 4). The electronic surface states may effectively change the topology of the sample, transforming a simply connected geometry (e.g., a solid cylinder or a disk) into a doubly connected one (e.g., a ring) where the AB effect may occur (see Refs. 5 and 6 and the reviews in Refs. 4, 7, and 8). In solids, the AB effect is manifested by an oscillatory dependence of the thermodynamic properties (magnetization or persistent current) and the transport (conductance) coefficients on the magnetic flux, with the period of the oscillations determined by the flux quantum $\phi_0 = hc/e$. The AB effect in various simply connected systems such as dots, wires, and quantum contacts has been studied quite extensively.[9–17]

In this paper we investigate the temperature dependence of magnetization oscillations (mainly the AB oscillations) in circularly symmetric or asymmetric quantum dots.[18] The dot is modeled by a (symmetric or asymmetric) harmonic confining potential, which allows us to obtain an expression for the spectrum of the electrons in the presence of an applied magnetic field, and to calculate analytically the magnetization of the dot. We demonstrate the existence of four different temperature scales of magnetization oscillations: (i) At low magnetic fields the AB oscillations and a (superimposed) oscillating fine structure (with oscillations of smaller period and amplitude), are characterized by the temperature scales $\hbar v_F/a$ and $\hbar^2/ma^2$, respectively, where v_F is the Fermi velocity of the electrons and m is the electronic mass. (ii) At high magnetic fields the de Haas–van Alphen oscillations and the AB oscillatory structure have temperature scales $\hbar\omega_c$ and $(\hbar v_F/a)(v_F/a\omega_c)$, respectively; the latter temperature scale for the AB oscillations is less than the one corresponding to the case of low magnetic fields. Additionally, we study the effects of the asymmetry of the confining potential on the magnetization in the limit of low temperatures and weak magnetic fields.

The paper is organized as follows. In Sec. II we discuss the model used for the description of the quantum dot, and calculate the magnetization both analytically and numerically. We summarize our results in Sec. III.

II. MODEL AND RESULTS

We study a dot formed in a two-dimensional electron gas with an asymmetric harmonic confining potential U_D,

$$U_D(x,y) = \frac{m}{2}(\omega_x^2 x^2 + \omega_y^2 y^2), \tag{1}$$

where m is the electronic mass and the characteristic confining frequencies $\omega_{x,y}$ may be related to the chemical potential

ζ and the effective size of the dot (L is the effective boundary of the dot) as

$$U_D(x,y)|_L = \zeta, \qquad (2a)$$

or, equivalently,

$$U_D(a_x,0) = U_D(0,a_y) = \zeta, \qquad (2b)$$

where a_x and a_y are the semimajor axes of the elliptical dot. Note that $\omega_{x,y} = v_F/a_{x,y}$.

We place the dot in a magnetic field perpendicular to the plane of the dot, and choose a symmetric gauge for the vector potential

$$\mathbf{A} = \tfrac{1}{2}(-Hy, Hx, 0). \qquad (3)$$

In this model the energy levels of the electrons in the dot are given by[19]

$$E_{n_1 n_2} = \hbar\omega_+(n_1 + \tfrac{1}{2}) + \hbar\omega_-(n_2 + \tfrac{1}{2}) \qquad (4)$$

and

$$\omega_\pm = \tfrac{1}{2}\left[\sqrt{\omega_c^2 + (\omega_x + \omega_y)^2} \pm \sqrt{\omega_c^2 + (\omega_x - \omega_y)^2}\right], \qquad (5)$$

where n_1 and n_2 are non-negative integers and $\omega_c = eH/mc$ is the cyclotron frequency. The energy levels $E_{n_1 n_2}$ given by Eqs. (4) and (5) transform to the Fock-Darwin levels[20] in the symmetric case ($\omega_x = \omega_y = \omega_0$), with

$$\omega_\pm^s = \tfrac{1}{2}(\sqrt{\omega_c^2 + 4\omega_0^2} \pm \omega_c). \qquad (6)$$

In a grand canonical ensemble (i.e., an ensemble characterized by a constant chemical potential) the magnetic properties are determined by the thermodynamic potential[21] Ω

$$\Omega = -2T \sum_{n_1 n_2} \ln[1 + e^{(\zeta - E_{n_1 n_2})/T}], \qquad (7)$$

where T is the absolute temperature (here we express T in units of energy with the Boltzmann constant $k_B = 1$). Introducing the density of states and integrating twice by parts, we obtain

$$\Omega = -\frac{1}{T} \int dE \, \frac{g(E) e^{(E-\zeta)/T}}{[1 + e^{(E-\zeta)/T}]^2}, \qquad (8)$$

where

$$g(E) = 2 \sum_{n_1 n_2} (E - E_{n_1 n_2}) \theta(E - E_{n_1 n_2}). \qquad (9)$$

Here $\theta(x)$ is the Heaviside θ function, and the multiplication by 2 is due to the electron spin.

Differentiation of the thermodynamic potential in Eq. (8) with respect to the magnetic field gives the magnetization of the quantum dot

$$M = -\frac{\partial\Omega}{\partial H}. \qquad (10)$$

Expressions (4), (5), and (8)–(10) allow us to calculate the magnetic response of the quantum dot. Successively applying the Poisson summation formula in the form

$$\sum_n f\left(n + \frac{1}{2}\right) = \sum_{k=-\infty}^{\infty} (-1)^k \int dn \, f(n) e^{2\pi i k n} \qquad (11)$$

to the double sum in Eq. (9), we obtain

$$\begin{aligned}
g(E) = {}& \frac{E^3}{3\hbar^2 \omega_x \omega_y} - \frac{E(\omega_x^2 + \omega_y^2 + \omega_c^2)}{12\omega_x \omega_y} + \frac{i\hbar\omega_+^2}{4\pi^3 \omega_-} \\
& \times \sum_{s=-\infty}^{\infty}{}' \; (-1)^s \frac{e^{2i\pi s E/\hbar\omega_+}}{s^3} + \frac{i\hbar\omega_-^2}{4\pi^3 \omega_+} \\
& \times \sum_{k=-\infty}^{\infty}{}' \; (-1)^k \frac{e^{2i\pi k E/\hbar\omega_-}}{k^3} + \frac{i\hbar}{4\pi^3} \\
& \times \sum_{k=-\infty}^{\infty}{}' \; (-1)^k \sum_{s=-\infty}^{\infty}{}' \; (-1)^s \\
& \times \frac{s^2 \omega_-^2 e^{2i\pi k E/\hbar\omega_-} - k^2 \omega_+^2 e^{2i\pi s E/\hbar\omega_+}}{k^2 s^2 (k\omega_+ - s\omega_-)}, \qquad (12)
\end{aligned}$$

where Σ' denotes summation excluding the terms $k=0$ and $s=0$.

Substituting the function $g(E)$ into Eq. (8), and integrating over the energy in the limit $T \ll \zeta$, for the thermodynamic potential we obtain the expression

$$\begin{aligned}
\Omega \approx {}& -\frac{\zeta^3}{3\hbar^2 \omega_x \omega_y} + \frac{1}{12}\zeta \frac{\omega_x^2 + \omega_y^2 + \omega_c^2}{\omega_x \omega_y} - \frac{i\hbar\omega_+^2}{4\pi^3 \omega_-} \sum_{s=-\infty}^{\infty}{}' \; (-1)^s \frac{e^{2i\pi s\zeta/\hbar\omega_+}}{s^3} \psi(2\pi^2 s T/\hbar\omega_+) \\
& -\frac{i\hbar\omega_-^2}{4\pi^3 \omega_+} \sum_{k=-\infty}^{\infty}{}' \; (-1)^k \frac{e^{2i\pi k\zeta/\hbar\omega_-}}{k^3} \psi(2\pi^2 k T/\hbar\omega_-) \\
& -\frac{i\hbar}{4\pi^3} \sum_{k=-\infty}^{\infty}{}' \; (-1)^k \sum_{s=-\infty}^{\infty}{}' \; \frac{(-1)^s}{k^2 s^2 (k\omega_+ - s\omega_-)} [s^2 \omega_-^2 e^{2i\pi k\zeta/\hbar\omega_-} \psi(2\pi^2 k T/\hbar\omega_-) \\
& -k^2 \omega_+^2 e^{2i\pi s\zeta/\hbar\omega_+} \psi(2\pi^2 s T/\hbar\omega_+)], \qquad (13)
\end{aligned}$$

where $\psi(x) = x/\sinh(x)$.

In the first approximation with respect to the parameter $\zeta/\hbar\omega_\pm$ we obtain the expressions for the monotonic and oscillatory terms of the magnetic moment:

$$M \approx -\frac{\zeta\omega_c^2}{6H\omega_x\omega_y} + \frac{\zeta}{2\pi^2\omega_-}\frac{\partial\omega_+}{\partial H}\sum_{s=-\infty}^{\infty}{}' \, (-1)^s\frac{e^{2i\pi s\zeta/\hbar\omega_+}}{s^2}\psi(2\pi^2 sT/\hbar\omega_+)$$

$$+ \frac{\zeta}{2\pi^2\omega_+}\frac{\partial\omega_-}{\partial H}\sum_{k=-\infty}^{\infty}{}' \, (-1)^k\frac{e^{2i\pi k\zeta/\hbar\omega_-}}{k^2}\psi(2\pi^2 kT/\hbar\omega_-)$$

$$+ \frac{\zeta}{2\pi^2}\sum_{k=-\infty}^{\infty}{}' \, \sum_{s=-\infty}^{\infty}{}' \, \frac{(-1)^{k+s}}{ks(k\omega_+ - s\omega_-)}\left[s\frac{\partial\omega_-}{\partial H}e^{2i\pi k\zeta/\hbar\omega_-}\psi(2\pi^2 kT/\hbar\omega_-) \right.$$

$$\left. - k\frac{\partial\omega_+}{\partial H}e^{2i\pi s\zeta/\hbar\omega_+}\psi(2\pi^2 sT/\hbar\omega_+)\right]. \tag{14}$$

The monotonic part of the magnetic moment [the first term on the right-hand side of Eq. (14)] describes the Landau diamagnetism of the dot. Taking into account Eq. (2b), for the non oscillatory part of the magnetic susceptibility we obtain $\chi = M/SH$, where $S = \pi ab$ is the effective area of the dot, the expression

$$\mathcal{X}_s = -\frac{e^2}{12\pi mc^2} = -\frac{1}{3}\beta_0^2\nu_s. \tag{15}$$

Here $\beta_0 = e\hbar/2mc$ is the Bohr magneton, and $\nu_s = m/\pi\hbar^2$ is the two-dimensional density of states. In the following we focus mostly on the oscillatory part of the magnetic moment and its temperature dependence.[22] The oscillations of the magnetization are described by the functions $\exp(2i\pi\zeta/\hbar\omega_\pm)$ and their combinations. The amplitudes of the magnetic oscillations decrease with increase of the temperature and at high temperatures they are exponentially small, i.e., $\psi(x) \approx e^{-x}$ for $x \gg 1$, where $x = 2\pi^2 T/\hbar\omega_\pm$. In the numerical calculations discussed below of the magnetic response of a dot formed in GaAs we use the data[4] $\varepsilon_F = 14$ meV and $v_F = 2.7 \times 10^7$ cm/s, and the electronic mass $m = 0.067m_0$.

A. Symmetric dot

First we analyze the magnetic response of a symmetric dot, i.e., a dot formed by a symmetric confining potential with $\omega_x = \omega_y = \omega_0$; we take $\zeta/\hbar\omega_0 = 70$, which corresponds to a dot with a radius $R \approx 0.8 \times 10^{-4}$ cm. In Fig. 1 we display the magnetic moment as a function of the strength of the applied magnetic field (expressed as ω_c/ω_0) for different values of the temperature (expressed in units of $\hbar\omega_0$, with the energy $\hbar\omega_0$ corresponding in our case to a temperature of 2.2 K). The magnetic moment exhibits a strong oscillatory behavior in the entire range of the magnetic-field strength. We analyze this behavior in detail below, both in the regime of weak ($\omega_c \ll \omega_0$) and strong ($\omega_c \gg \omega_0$) magnetic fields.

Weak magnetic fields

Since in a weak magnetic field the frequencies of the electronic motion can be written as $\omega_\pm \approx \omega_0 \pm \omega_c/2$, the func-

tions $\zeta/\hbar\omega_\pm$ that enter the expression determining the oscillatory dependence of the magnetization [see Eq. (14)] have the form

$$\zeta/\hbar\omega_\pm \approx (\zeta/\hbar\omega_0)(1 \mp \omega_c/2\omega_0). \tag{16}$$

The first term on the right-hand-side $\zeta/\hbar\omega_0 = k_F R/2$, where k_F is the Fermi wave number, describes quantum size oscillations due to the harmonic confinement potential. The second term on the right $\zeta\omega_c/2\hbar\omega_0^2 = \pi R^2 H/2(hc/e)$, is respon-
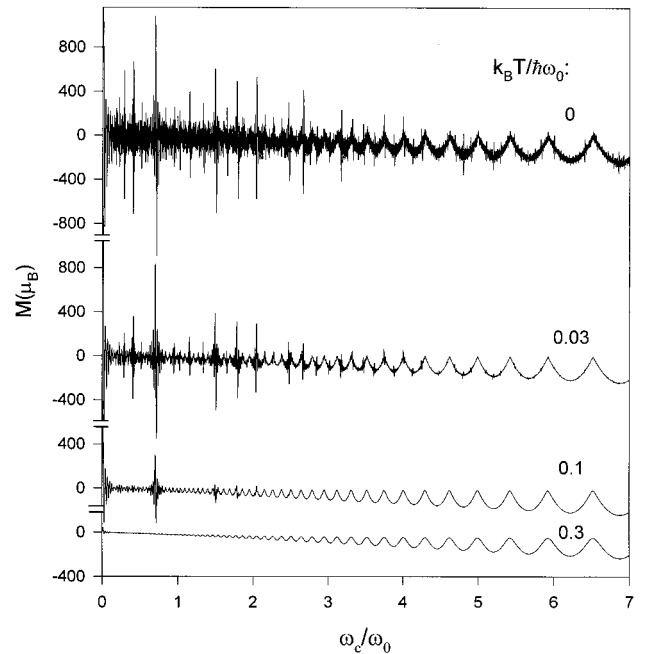
FIG. 1. The magnetization (in units of the Bohr magneton μ_B) of a symmetric quantum dot displayed as a function of the magnetic field (in dimensionless units of ω_c/ω_0, where ω_c is the cyclotron frequency and $\omega_0 = v_F/R$ with R the effective radius of the dot), plotted for various values of the temperature (T, in units of $\hbar\omega_0$). In our calculations we used $\zeta/\hbar\omega_0 = 70$ which corresponds to approximately 2500 electrons in the dot. Note that the AB oscillations vanish first in the region of strong magnetic fields (see text).
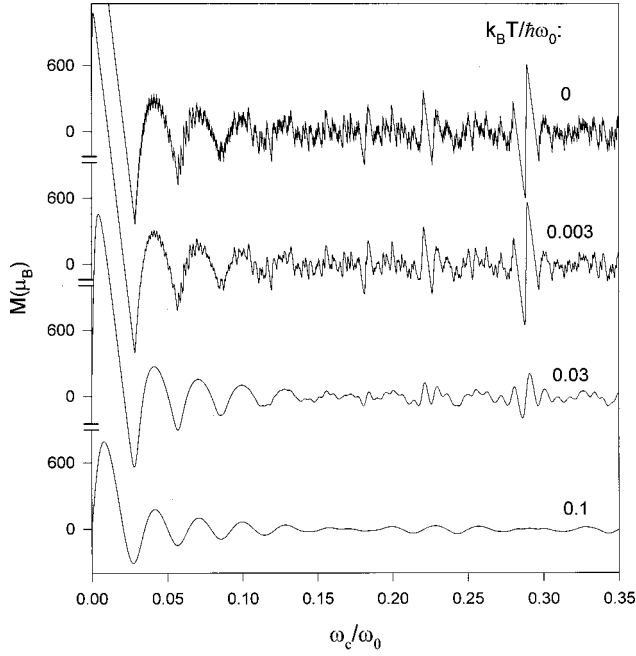
FIG. 2. Same as in Fig. 1, but focusing on the region of weak magnetic fields ($\omega_c \ll \omega_0$). Note that the superfine structure ("grass" superimposed on the AB oscillations) fluctuating with a "period" of the order of $(hc/e)/k_F R$, vanishes at high temperatures.

FIG. 3. Same as in Fig. 2, but in the region of strong magnetic fields ($\omega_c \gg \omega_0$). Note that the AB oscillations superimposed on the de Haas–van Alphen ones vanish at high temperatures.

sible for the AB oscillations; the factor 2 in the period of the AB oscillations is due to the chosen harmonic confining potential model [see Eqs. (1) and (2a)]; compare with the proper AB period, hc/e, of the oscillations in the limit of weak fields in simply connected systems with a hard wall confining potential[2]. Note that using quantum mechanical definition of the average square of the effective radius $\langle R_{\mathrm{eff}}^2 \rangle = R^2/2$ we can restore the proper AB period of oscillations, hc/e.

The temperature decay of the AB oscillations is described by $e^{-2\pi^2 T/\hbar\omega_0}$ [the ψ function in Eq. (14)] and the temperature scale of the decay ($\hbar\omega_0 = \hbar v_F/R$) does not depend on the magnetic field because in a weak magnetic field the electronic states are formed by the confining potential. The dependence of the magnetic moment on the magnetic field in the limit $\omega_c/\omega_0 \ll 1$, is shown in Fig. 2 for different temperatures. It is of interest to note that in addition to the AB oscillations there appears a superimposed superfine fluctuating structure ("grass") with a "period" of the order of $(hc/e)/k_F R$, that is caused by magnetic-field-induced shifts of the electronic levels through the Fermi level (compare with a similar fine structure occurring in the conductance and thermopower of nanowires[13,23]). The temperature scale of such mesoscopic oscillations is ϵ_F/N (N is the number of electronic states in the dot) which in our model is of the order of $(\hbar\omega_0)^2/\epsilon_F \approx 2\hbar^2/mR^2$. The ratio of the temperature scales of the AB oscillations and the superfine oscillating structure is of the order of $\zeta/\hbar\omega_0$. An increase of the temperature smears the fine structure and restores the "pure" AB oscillations (see the two bottom curves in Fig. 2). At very low temperatures and in an extremely weak magnetic

field the magnetization exhibits a paramagnetic behavior[24,25] (see the upper curve in Fig. 2 for $\omega_c/\omega_0 < 0.0025$). Such a strong paramagnetic "singularity" is due to the high degree of degeneracy of the electronic energy levels in a quantum dot modeled by a symmetric harmonic confining potential (see below).

Strong magnetic fields

In a strong magnetic field magnetic quantization starts to dominate. In this limit $\omega_+ \approx \omega_c$, and $\omega_- \approx \omega_0^2/\omega_c$, and for the functions $\zeta/\hbar\omega_\pm$ we have

$$\frac{\zeta}{\hbar\omega_+} \approx \frac{\zeta}{\hbar\omega_c} \tag{17a}$$

and

$$\frac{\zeta}{\hbar\omega_-} \approx \frac{\pi R^2 H}{hc/e}. \tag{17b}$$

These functions describe the de Haas–van Alphen [Eq. (17a)] and the AB [Eq. (17b)] effects, with the AB oscillations superimposed on the de Haas–van Aplhen structure (see Fig. 3).[9,10,15,26] The temperature scales of the de Haas–van Alphen and AB effects are $\hbar\omega_c$ and $\hbar\omega_0^2/\omega_c$, respectively; the latter depends on the magnetic field and differs from the corresponding temperature scale ($\hbar\omega_0$) for the AB effect in the case of weak fields. Note that with increase of the temperature the AB oscillations vanish first in the strong-field region (at $T \gtrsim \hbar\omega_0^2/\omega_c$), and then (at $T \gtrsim \hbar\omega_0$) in the weak-field region (see Fig. 1). A similar effect, pertaining to different scales characterizing the temperature decay of AB oscillations in the conductance of nanowires has been discussed in Ref. 16.

B. Asymmetric dot

To study effects caused by the asymmetry of a quantum dot we employ a confining potential with $\omega_x \neq \omega_y$ [see Eq. (1)]. The effects of the asymmetry of the dot on the magnetic oscillations are more pronounced in the weak-magnetic-field region, i.e., when the size of the dot is comparable with the cyclotron radius. In Fig. 4 we display the magnetic moment of an asymmetric dot as a function of the magnetic field (expressed as ω_c/ω_0) for different values of ω_x/ω_y, while

maintaining a constant value for the area of the dot, i.e., $\omega_x \omega_y$ is held constant.

We now analyze the dependence of the magnetic moment of the quantum dot on the chemical potential ζ and the influence of the anisotropy of the confining potential on the magnetic moment in the regime of low temperatures and weak magnetic fields. After simple algebraic transformations, the expression for the magnetic moment [Eqs. (7) and (10)] may be rewritten as

$$
M = -2\mu_B \frac{\omega_c}{\sqrt{\omega_c^2 + \omega_0^2(\alpha^2 + 4)}} \sum_{\substack{n_1 \geqslant 0 \\ n_2 \geqslant 0}} (n_1 + n_2 + 1) \frac{1}{1 + \exp\left(\dfrac{E_{n_1 n_2} - \zeta}{T}\right)}
$$

$$
+ 2\mu_B \frac{\omega_c}{\sqrt{\omega_c^2 + \alpha^2 \omega_0^2}} \sum_{\substack{n_1 > 0 \\ n_1 > n_2 \geqslant 0}} (n_1 - n_2) \frac{\exp\left(\dfrac{E_{n_1 n_2} - \zeta}{T}\right) - \exp\left(\dfrac{E_{n_2 n_1} - \zeta}{T}\right)}{\left[1 + \exp\left(\dfrac{E_{n_1 n_2} - \zeta}{T}\right)\right]\left[1 + \exp\left(\dfrac{E_{n_2 n_1} - \zeta}{T}\right)\right]}, \tag{18}
$$

where $\alpha = (\omega_y - \omega_x)/\omega_0$ is the dimensionless parameter defining the anisotropy of the confining potential. In the following we consider the case of weak magnetic fields ($\omega_c/\omega_0 \ll 1$) and the small anisotropy of the confining potential ($\alpha \ll 1$). The first term on the right in Eq. (18) describes a diamagnetic background of the magnetic moment, and in the low-temperature regime it is of the order of $(\mu_B/3) \times (\zeta/\hbar\omega_0)^3(\omega_c/\omega_0)$. For a small anisotropy the diamagnetic background does not depend on α, and it is proportional to the strength of the magnetic field (Landau diamagnetism). The second term in Eq. (18) describes paramagnetic peaks in the magnetic moment, occurring when the chemical potential coincides with the energy level $E_{n_1 n_2}|_{H=0}$. The heights of the paramagnetic peaks are of the order of $\frac{1}{2}(\omega_c/\sqrt{\omega_c^2 + \alpha^2 \omega_0^2})(\zeta/\hbar\omega_0)^2$, and for a cylindrically symmetric confining potential (i.e., $\alpha = 0$) they do not depend on the magnetic field. Note that in the low temperature regime neither the diamagnetic background nor the heights of the paramagnetic peaks depend on the temperature.

To illustrate the above analysis, in Fig. 5 we show the behavior of the magnetic moment of the dot in the low-temperature regime ($T \ll \hbar\omega_0$) as a function of the dimensionless parameter $\zeta/\hbar\omega_0$, for various values of the anisotropy parameter α and the strength of the magnetic field characterized by ω_c/ω_0. As in the previous figure, the change of the shape of the confining potential is performed while keeping the area of the dot constant, i.e., $(\omega_x \omega_y)^{1/2} = \omega_0 = \text{const}$. The magnetic moment of the dot exhibits a series of paramagnetic peaks superimposed on a diamagnetic background. Paramagnetic peaks occur when $\zeta = E_{n_1 n_2}$, i.e., when $\zeta/\hbar\omega_0$ is an integer number. The peaks are more pronounced in the case of weak magnetic fields [compare Figs.

5(a) and 5(b)] and small asymmetry [compare different curves corresponding to different values of the asymmetry parameter α in Fig. 5(a)]. The heights of the peaks increase as $(\zeta/\hbar\omega_0)^2/2$, with an increase of the value of $\zeta/\hbar\omega_0$, and in the case of a symmetric dot they do not depend on the magnetic-field strength [compare the curves corresponding to $\alpha = 0$ in Figs. 5(a) and 5(b)]. On the other hand, in an
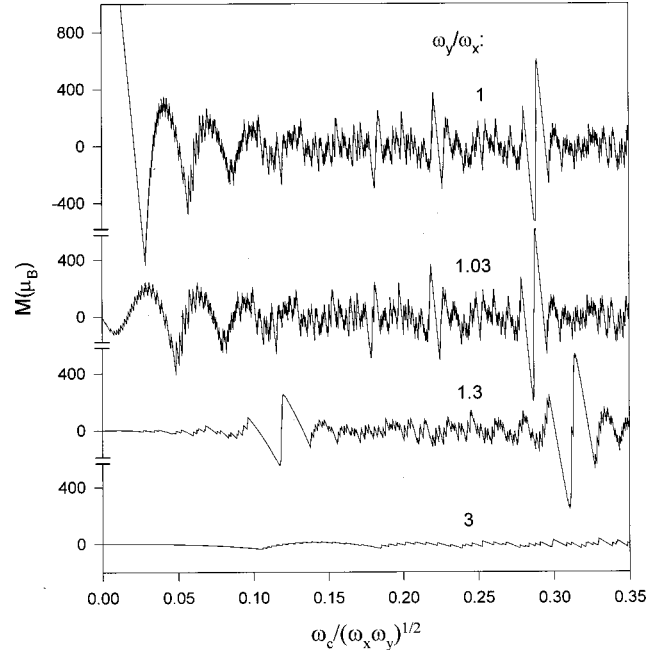
FIG. 4. The magnetization (in units of μ_B) of an asymmetric quantum dot displayed as a function of the magnetic field (in dimensionless units of ω_c/ω_0), plotted for different values of ω_x/ω_y. The area of the dot, i.e., $\omega_x \omega_y$, is held constant.
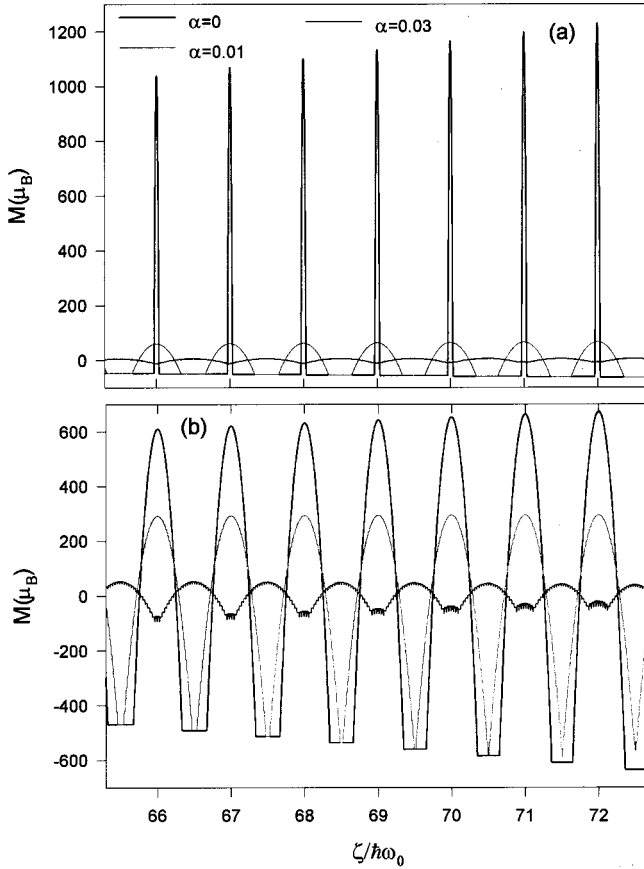
FIG. 5. The magnetization (in units of μ_B) of an asymmetric quantum dot displayed as a function of $\zeta/\hbar\omega_0$, plotted in the low-temperature limit ($T=0.001\hbar\omega_0$) for several values of the asymmetry parameter $\alpha=(\omega_x-\omega_y)/\omega_0$ and for different magnetic fields [$\omega_c/\omega_0=0.001$ in (a) and $\omega_c/\omega_0=0.01$ in (b)]. Note the decrease and smearing of the paramagnetic peaks of the magnetization with increase of the asymmetry parameter α.

strong oscillatory behavior as a function of the magnetic field (Fig. 1), and the decay of the oscillations as a function of the temperature is characterized by four temperature scales.

(i) At low magnetic fields, $\omega_c \ll \omega_0$, the occurrence of AB oscillations is accompanied by a superimposed fine structure (grass) (Fig. 2). The temperature scales of these oscillations are

$$\Delta_{\mathrm{AB}}^L \sim \frac{\hbar v_F}{R} \sim \hbar\omega_0 \qquad (19)$$

and

$$\Delta_{\mathrm{grass}}^L \sim \frac{\varepsilon_F}{N} \sim \hbar\omega_0 \frac{\hbar\omega_0}{\varepsilon_F}, \qquad (20)$$

respectively. The AB oscillations are associated with the electronic states localized near the surface of the dot (the analog of whispering gallery states) and their temperature scale [Eq. (19)] is determined by the spacing between the surface energy levels. The grass is caused by magnetic-field-induced shifts of the energy levels through the Fermi energy, and its temperature scale, [Eq. (20)] is of the order of the average spacing between the quantized energy levels in the dot. Note that both temperature scales do not depend on the magnetic field in the region of weak fields.

(ii) At high magnetic fields, $\omega_c \gg \omega_0$, the AB oscillations are superimposed on the de Haas–van Alphen ones (Fig. 3). Their temperature scales are

$$\Delta_{\mathrm{AB}}^H \sim \frac{\hbar\omega_0^2}{\omega_c} \qquad (21)$$

and

$$\Delta_{\mathrm{dH}\nu\mathrm{A}}^H \sim \hbar\omega_c, \qquad (22)$$

respectively. In this case the AB oscillations are due to edge states of the dot and their temperature scale. [Eq. (21)] is much smaller than in the weak magnetic fields regime, [Eq. (19)] and it is strongly dependent on the magnetic-field strength. Finally, we note that an asymmetry of the quantum dot influences in a substantial way both the oscillatory part of the magnetization (Fig. 4) and its steady part (paramagnetic peaks superimposed on a diamagnetic background) in the limit of low temperature and weak magnetic fields (Fig. 5).

asymmetric dot the magnetic field may significantly influence the heights of paramagnetic peaks [compare the curves corresponding to $\alpha=0.01$ in Figs. 5(a) and 5(b)] as the amplitude of the peaks is proportional to $\omega_c/\sqrt{\omega_c^2+\alpha^2\omega_0^2}$ (see above). The width of the peaks depends strongly on the asymmetry of the dot as well as on the strength of the magnetic field as the electronic energy levels, which are highly degenerate in a symmetric harmonic confining potential in the absence of the magnetic field, split under the influence of the magnetic field, and the asymmetry of the potential. The diamagnetic background is proportional to the magnetic-field strength; note the increase in the magnitude of the diamagnetic background in Fig. 5(b) compared to the one in Fig. 5(a), exhibiting a $(\zeta/\hbar\omega_0)^3$ dependence.

III. SUMMARY

In this paper we have studied the magnetization of a circularly symmetric and asymmetric quantum dot modeled by a harmonic confining potential. The magnetization exhibits a

ACKNOWLEDGMENTS

[1] Y. Aharonov and D. Bohm, Phys. Rev. **115**, 485 (1959).

[2] E. N. Bogachek and G. A. Gogadze, Zh. Eksp. Teor. Fiz. **63**, 1839 (1972) [Sov. Phys. JETP **36**, 973 (1973)]; E. N. Bogachek, Fiz. Nizk. Temp. **2**, 473 (1976) [Sov. J. Low Temp. Phys. **2**, 235 (1976)].

[3] N. B. Brandt, D. V. Gitsu, A. A. Nikolaeva, and Ya. G. Ponomarev, Pis'ma Zh. Eksp. Teor. Fiz. **24**, 304 (1976) [JETP Lett. **24**, 272 (1976)]; N. B. Brandt, E. N. Bogachek, D. V. Gitsu, G. A. Gogadze, I. O. Kulik, A. A. Nikolaeva, and Ya. G. Ponomarev, Fiz. Nizk. Temp. **8**, 718 (1982) [Sov. J. Low Temp. Phys. **8**, 358 (1982)].

[4] C. W. J. Beenakker and H. van Houten, in *Solid State Physics*, edited by H. Ehrenreich and D. Turnbull (Academic, San Diego, 1991), Vol. 44, p. 1.

[5] N. Byers and C. N. Yang, Phys. Rev. Lett. **7**, 46 (1961).

[6] I. O. Kulik, Pis'ma Zh. Eksp. Teor. Fiz. **11**, 407 (1970) [JETP Lett. **11**, 275 (1970)].

[7] S. Washburn and R. A. Webb, Adv. Phys. **35**, 375 (1986).

[8] E. N. Bogachek and I. O. Kulik, in *Progress in High Temperature Superconductivity*, edited by A. Barone and A. Larkin (World Scientific, Singapore, 1987), Vol. 4, p. 80.

[9] U. Sivan and Y. Imry, Phys. Rev. Lett. **61**, 1001 (1988).

[10] Y. Meir, O. Entin-Wohlman, and Y. Gefen, Phys. Rev. B **42**, 8351 (1990).

[11] P. H. M. van Loosdrecht, C. W. J. Beenaker, H. van Houten, J. G. Williamson, B. J. van Wees, J. E. Mooij, C. T. Foxon, and J. J. Harris, Phys. Rev. B **38**, 10 162 (1988).

[12] L. I. Glazman and M. Jonson, Phys. Rev. B **41**, 10 686 (1990).

[13] E. N. Bogachek, M. Jonson, R. I. Shekhter, and T. Swahn, Phys. Rev. B **47**, 16 635 (1993); **50**, 18 341 (1994).

[14] E. N. Bogachek and U. Landman, Phys. Rev. B **50**, 2678 (1994).

[15] E. N. Bogachek and U. Landman, Phys. Rev. B **52**, 14 067 (1995).

[16] A. G. Scherbakov, E. N. Bogachek, and U. Landman, Phys. Rev. B **53**, 4054 (1996).

[17] N. G. Galkin, V. A. Geyler, and V. A. Margulis, Zh. Eksp. Teor. Fiz. **117**, 593 (2000) [JETP **90**, 517 (2000)].

[18] A preliminary report on this subject was presented by A. G. Scherbakov, E. N. Bogachek, and U. Landman, Bull. Am. Phys. Soc. **41**, No. 1, 553 (1996).

[19] B. Schuh, J. Phys. A **18**, 803 (1985).

[20] V. Fock, Z. Phys. **47**, 446 (1928); C. G. Darwin, Proc. Cambridge Philos. Soc. **27**, 86 (1930).

[21] L. D. Landau and E. M. Lifshitz, *Statistical Physics* (Pergamon Press, Oxford, 1980), Pt. 1.

[22] Some aspects of the energy (temperature) scales in orbital magnetism in different two-dimensional integrable systems were discussed by E. Gurevich and B. Shapiro, J. Phys. I **7**, 807 (1997).

[23] E. N. Bogachek, A. G. Scherbakov, and U. Landman, Phys. Rev. B **54**, R11 094 (1996).

[24] F. Meir and P. Wyder, Phys. Rev. Lett. **30**, 181 (1973).

[25] A. I. Buzdin, O. V. Dolgov, and Yu. E. Lozovik, Phys. Lett. **100A**, 261 (1984).

[26] E. N. Bogachek and I. O. Kulik, Fiz. Nizk. Temp. **9**, 398 (1983) [Sov. J. Low Temp. Phys. **9**, 202 (1983)].